AIAA JOURNAL
Vol. 44, No. 7, July 2006

# Analysis of Edge Effect in Large Deflections of Rotationally Symmetric Membrane Caps

J. Joseph*
*Fleetguard/Nelson, Cookeville, Tennessee 38502*
and
J. Peddieson† and G. Ramirez‡
*Tennessee Technological University, Cookeville, Tennessee 38505*

**An analysis of the edge effect in rotationally symmetric membrane caps is carried out using equations correct for arbitrarily large deflections. General closed-form solutions are obtained and used to demonstrate the protection of the interior membrane shape from edge deflections observed in numerical solutions reported in the literature. An alternative asymptotic analysis is also discussed.**

## Nomenclature

| | | |
|---|---|---|
| $c$ | = | constant of integration |
| $D$ | = | diameter |
| $E$ | = | Young's modulus |
| $e_r$ | = | radial engineering strain |
| $e_\theta$ | = | transverse engineering strain |
| $F$ | = | edge effect stress function |
| $f$ | = | focal length |
| $h$ | = | membrane thickness |
| $I_0$ | = | zeroth-order modified Bessel function of first kind |
| $I_1$ | = | first-order modified Bessel function of first kind |
| $q$ | = | axial force per projected area |
| $q_r$ | = | radial force per undeformed area |
| $q_z$ | = | axial force per undeformed area |
| $q_0$ | = | maximum axial loading intensity |
| $r$ | = | radial polar coordinate |
| $T_r$ | = | Lagrangian radial stress resultant |
| $T_\theta$ | = | Lagrangian transverse stress resultant |
| $T_0$ | = | boundary load |
| $u$ | = | radial displacement |
| $u_0$ | = | boundary displacement |
| $V$ | = | Lagrangian axial stress resultant |
| $W$ | = | rigid axial displacement |
| $w$ | = | axial displacement |
| $z$ | = | axial polar coordinate |
| $z_0$ | = | maximum membrane height |
| $\alpha$ | = | load parameter |
| $\beta$ | = | geometric parameter |
| $\Delta$ | = | cap depth parameter |
| $\Delta R/R$ | = | boundary-displacement parameter |
| $\Delta\psi$ | = | stress function perturbation |
| $\varepsilon$ | = | cap depth/loading intensity parameter |
| $\theta$ | = | transverse polar coordinate |
| $\xi$ | = | edge effect coordinate |
| $\nu$ | = | Poisson's ratio |
| $\sigma_{\text{ctr}}$ | = | nominal central stress |
| $\psi$ | = | stress function |
| $'$ | = | derivative with respect to $r$ |
| $\circ$ | = | derivative with respect to $\xi$ |

Received 5 May 2004; revision received 21 December 2005; accepted for publication 26 December 2005. 

*Mechanical Engineer.
†Professor of Mechanical Engineering; jpeddieson@tntech.edu.
‡Assistant Professor of Civil and Environmental Engineering.

## Introduction

LARGE deployable space structures are of interest for use as solar collectors and concentrators, radio frequency and optical reflectors, and microwave antennas, among other devices. Such structures often exhibit negligible bending stiffness and, therefore, can be regarded as membranes. Furthermore, such structures typically undergo large deflections. An example of the application of membrane analysis to a current aerospace related problem is provided by the recent paper by Greschik et al.[1] Several other examples are supplied by the references contained therein.

The problem of predicting the large deflection behavior of membranes was of interest long before the space age. This is both because of applications, such as the proposed use of inflatable domes as portable structures during World War II (Bromberg and Stoker[2]) and because this problem is inherently nonlinear and, as such, constitutes one of the simplest model problems associated with nonlinear plate and shell analysis.

The study of large deformations of axisymmetric membranes was initiated by Hencky[3] with contributions continuing to appear until the present. A representative sample is provided by Refs. 1 and 2; the papers of Reissner,[4] Dickey,[5–8] Yang and Feng,[9] Smith et al.,[10] Chang and Peddieson,[11] Fan and Peddieson,[12] Foroutan-Naini and Peddieson,[13] Tseng and Peddieson,[14] Kyriakides and Chang,[15] Khayat et al.,[16] Foroudastan and Peddieson,[17] Weinitschke and Grabmüller,[18] Khayat and Derdouri,[19] and Beck and Grabmüller[20]; the report by Rossettos[21]; and the references cited therein. An edge effect has been observed for initially curved axisymmetric membranes. For certain parametric combinations the familiar linear membrane solution (for instance, by Kraus[22]) is found to hold everywhere except in the vicinity of a fixed boundary, where deviations must occur to satisfy the boundary conditions. This can be observed in numerical results (for instance, in Refs. 1 and 16) and has also been addressed analytically in Refs. 2, 4, 10, 11, 17, and 21. All analytical work has been based on equations limited to moderately large deflections.

The present paper reports an analysis of the edge effect based on a formulation that is correct for arbitrarily large deflections of a class of axisymmetric membranes. The simplified equations governing a uniformly valid first approximation are derived and a closed-form solution of these equations is obtained. It is shown that this solution provides another manifestation of the phenomenon of protection of the interior shape of the deflected membrane from edge displacements illustrated by the numerical solutions of Greschik et al.[1] An alternative (and complementary) approach to analysis of the edge effect, which generalizes an idea of Dickey,[7] is also presented.

Note that, whereas the literature on large deflections of membranes is extensive, the part pertaining to analytical description of the edge effect in caps is not. In fact, to the knowledge of the present authors, only five publications[2,4,10,11,21] have addressed this

topic since 1945. Of these, none are based of equations correct for arbitrarily large deflections, none deal with other than spherical or conical geometries, only one[21] addresses deep caps, and only two[2,10] appear in journals.

Because of the lack of publications on analytical description of the discussed edge effect, Ref. 7 is a welcome addition to the literature. Although the edge effect is not explicitly mentioned therein, it is inherent in the analysis. This work (like Refs. 2, 4, 10, and 11) is limited to moderately large deflections of shallow caps. It was felt, therefore, to be of interest to both extend this analysis to the same level of generality as the edge effect analysis reported herein and demonstrate the connection between the two.

The significance of the present paper is as follows. First, it bases edge effect analysis on equations correct for arbitrarily large deflections. Second, it reports a compact (stress function-based) formulation of the edge effect equations for deep caps. Third, it presents a closed-form solution that is pertinent to configurations other than spherical and conical. This solution provides an analytical example of the shape protection phenomenon observed in previous numerical investigations. Fourth, it extends the alternate asymptotic analysis of Ref. 7 to equations correct for arbitrarily large deflections and makes explicit the connection between this approach and the classical edge effect analysis. All of these things are done (apparently) for the first time.

## Formulation

Figure 1 shows a membrane cap (to borrow the terminology of Dickey[6]) that is rotationally symmetric with respect to $z$. It is convenient to describe the shape of a cap by regarding the polar coordinate $r$ as the independent variable and expressing the axial polar coordinate $z$ as a function of $r$ as shown.

Many equivalent alternative formulations of the equations describing arbitrarily large deflections of membrane caps are available. The present discussion is based on a combination of the formulations reported by Greschik et al.[1] and Dickey.[6–8]

If the engineering strains defined in Ref. 1 are expressed in terms of the displacements defined in Ref. 6, the results are the strain/displacement equations

$$e_r = \{[(1+u')^2 + (z'+w')^2]/(1+z'^2)\}^{\frac{1}{2}} - 1 \tag{1a}$$

$$e_\theta = u/r \tag{1b}$$

Greschik et al.[1] characterize the mechanical response using constitutive equations that relate the engineering strains to the Lagrangian (first Poila/Kirchhoff) stress resultants. Strain/stress resultant equations of this kind have the general forms

$$e_r = e_r(T_r, T_\theta), \qquad e_\theta = e_\theta(T_r, T_\theta) \tag{2}$$

If the respective radial and axial equilibrium equations of Ref. 6 are written in terms of the Lagrangian stress resultants, the results are

$$\left\{r(1+u')T_r \Big/ [(1+u')^2 + (z'+w')^2]^{\frac{1}{2}}\right\}' + (1+z'^2)^{\frac{1}{2}}(rq_r - T_\theta) = 0 \tag{3a}$$

$$\left\{r(z'+w')T_r \Big/ [(1+u')^2 + (z'+w')^2]^{\frac{1}{2}}\right\}' + (1+z'^2)^{\frac{1}{2}} rq_z = 0 \tag{3b}$$

Equations (1–3) contain six unknowns and, thus, constitute a determinate system.

When the surface loads are given per unit of undeformed area, it is sometimes convenient to employ an alternate formulation involving a stress function such that

$$\psi = r(1+u')T_r \Big/ [(1+u')^2 + (z'+w')^2]^{\frac{1}{2}}$$

$$\psi' = (1+z'^2)^{\frac{1}{2}}(T_\theta - rq_r) \tag{4}$$

which satisfies Eq. (3a) identically. Defining an axial stress resultant

$$V = (z'+w')T_r \Big/ [(1+u')^2 + (z'+w')^2]^{\frac{1}{2}} \tag{5}$$

and rearranging Eqs. (4) and (5) yields

$$T_r = [\psi^2 + (rV)^2]^{\frac{1}{2}}/r, \qquad T_\theta = \psi'/(1+z'^2)^{\frac{1}{2}} + rq_r \tag{6}$$

$$(1+u')/[(1+u')^2 + (z'+w')^2]^{\frac{1}{2}} = \psi/[\psi^2 + (rV)^2]^{\frac{1}{2}} \tag{7}$$

Substituting Eq. (5) into Eq. (3b), integrating once with respect to $r$, and enforcing regularity at $r = 0$ produces

$$V = -\left[\int_0^r (1+z'^2)^{\frac{1}{2}} rq_z \, dr\right] \Big/ r \tag{8}$$

Equation (1a) can be rearranged with the aid of Eq. (7) to read

$$(1+e_r)\psi \Big/ [\psi^2 + (rV)^2]^{\frac{1}{2}} = (1+u')/(1+z'^2)^{\frac{1}{2}} \tag{9}$$

Using Eq. (1b) to eliminate $u$ in favor of $e_r$ in Eq. (9) and rearranging the result yields

$$(re_\theta)' - (1+z'^2)^{\frac{1}{2}}\psi(1+e_r) \Big/ [\psi^2 + (rV)^2]^{\frac{1}{2}} + 1 = 0 \tag{10}$$

which plays a role similar to that of a compatibility equation. Because $q_r$ and $q_z$ are known functions of $r$ (surface loads given per unit of undeformed area), Eqs. (2), (6), (8), and (10) can be combined to create a single second-order differential equation with $\psi$ as dependent variable. This compact formulation, correct for arbitrarily large deflections, has been achieved at the expense of omitting from consideration some important loadings (such as pressures) that cannot be described per unit of undeformed area in terms of $r$ alone.

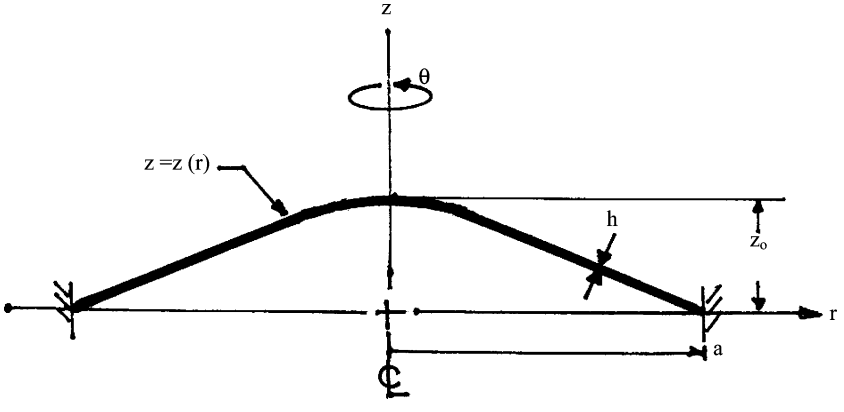


**Fig. 1 Geometry and coordinate system.**

For moderately large deflections, of course, the distinction between loads per unit of deformed and undeformed area disappears (as does the distinction between various types of stress resultants). Thus, the moderately large deflection version of Eqs. (1–10) can be thought of as an extension to deep caps of the compact stress function formulation reported previously for shallow caps.

## Edge Effect Analysis

A number of powerful numerical methodologies, such as the AM code (for axisymmetric deformations and geometries) discussed by Greschik et al.[1] and the FAIM code discussed by Palisoc and Huang,[23] are available for the solution of nonlinear membrane problems involving general shapes and loadings. Edge effect analysis, by its very nature, is not general but is meant to apply to a limited set of shapes and loadings. As discussed in Ref. 1, the difficult numerics of nonlinear membrane simulations make verification an important issue, especially for high-precision applications. Numerical problems are to be anticipated when edge effects exist because of the associated rapid changes of variables over small distances. It is believed that the most important role of edge effect analysis currently is not as an independent simulation tool, but as a contribution to verification of numerical methods. For this reason, simplifications have been made in the present work, which reduce generality to maximize the amount of closed-form solutions obtainable in a simple manner. These simplifications are to limit the forms of strain/stress resultant equations considered [Eqs. (2)] to those consistent with Hooke's law for plane stress:

$$e_r = (T_r - \nu T_\theta)/(Eh) \tag{11a}$$

$$e_\theta = (T_\theta - \nu T_r)/(Eh) \tag{11b}$$

(thus eliminating the consideration of wrinkling) and to limit the surface loadings considered to axial loads per unit of projected area on the $r$, $\theta$ plane:

$$q_r = 0, \qquad q_z = q/(1 + z'^2)^{\frac{1}{2}} \tag{12}$$

Although the present analysis cannot handle all loadings and constitutive equations, general purpose codes presumably can. Thus, these codes can be used to solve problems of the types described herein, and the numerical results can be compared with the closed-form solutions to be presented subsequently. In this way, the amount of grid refinement needed to resolve edge effects can be evaluated in a rational way. Whether the problems employed in this verification process are completely realistic is not of the utmost importance.

Substituting Eqs. (12) into Eqs. (6) produces

$$T_r = [\psi^2 + (rV)^2]^{\frac{1}{2}}/r, \qquad T_\theta = \psi'/m \tag{13}$$

where

$$m = (1 + z'^2)^{\frac{1}{2}} \tag{14}$$

Substituting Eqs. (13) into Eqs. (11) and combining the results with Eqs. (8), (10), and (14) leads to

$$\psi'' + (1/r - m'/m)\psi' - m^2\psi/r^2 + m\big(Eh\{1 - m\psi/[\psi^2 + (rV)^2]^{\frac{1}{2}}\}$$
$$- \nu[(rV)^2]'/\{2[\psi^2 + (rV)^2]^{\frac{1}{2}}\}\big)/r = 0 \tag{15}$$

where

$$V = -\left(\int_0^r rq\,\mathrm{d}r\right)\Big/ r \tag{16}$$

Combining Eqs. (1b), (11b), and (13) produces

$$u = \{r\psi'/m - \nu[\psi^2 + (rV)^2]^{\frac{1}{2}}\}/(Eh) \tag{17}$$

whereas combining Eqs. (1a), (11a), and (13) yields

$$w' = \big\{\big[m^2\big(1 + \{[\psi^2 + (rV)^2]^{\frac{1}{2}} - \nu r\psi'/m\}/(Ehr)\big)\big]^2$$
$$- (1 + u')^2\big\}^{\frac{1}{2}} - z' \tag{18}$$

Once $\psi$ is obtained from solving Eq. (15), the stress resultants are found from Eqs. (13), the radial displacement is found from Eq. (17), and the axial displacement is found by integrating Eq. (18) once.

Subsequent work will be facilitated by expressing Eqs. (13–18) in dimensionless forms. This is accomplished by introducing dimensionless variables (denoted by superposed asterisks) through the equations

$$r = ar^*, \qquad z = \Delta a z^*, \qquad V = V_0 V^*, \qquad q = V_0 q^*/a$$
$$\psi = V_0 a\psi^*/\Delta, \qquad T_r = V_0 T_r^*/\Delta, \qquad T_\theta = V_0 T_\theta^*/\Delta$$
$$u = a\Delta^2\varepsilon^2 u^*, \qquad w = a\Delta\varepsilon^2 w^* \tag{19}$$

where

$$\Delta = z_0/a \tag{20a}$$

$$\varepsilon = \left[V_0/(Eh\Delta^3)\right]^{\frac{1}{2}} \tag{20b}$$

The parameter $\Delta$ measures the depth of the cap ($\Delta \ll 1$ corresponding to a shallow cap), whereas the parameter $\varepsilon$ measures a combination of loading intensity and depth ($\varepsilon \ll 1$ corresponding to a combination of low loading and large depth).

Substituting Eqs. (19) into Eqs. (13–18) (and, for simplicity, dropping the superposed asterisks with the understanding that all subsequent equations are written in terms of dimensionless quantities) leads to

$$\varepsilon^2[\psi'' + (1/r - m'/m)\psi' - m^2\psi/r^2]$$
$$+ m\big(\{1 - m\psi/[\psi^2 + \Delta^2(rV)^2]^{\frac{1}{2}}\}/\Delta^2$$
$$- \nu\varepsilon^2\Delta^2[(rV)^2]'/\{2[\psi^2 + \Delta^2(rV)^2]^{\frac{1}{2}}\}\big)/r = 0 \tag{21a}$$

$$T_r = [\psi^2 + \Delta^2(rV)^2]^{\frac{1}{2}}/r \tag{21b}$$

$$T_\theta = \psi'/m \tag{21c}$$

$$u = r\psi'/m - \nu[\psi^2 + \Delta^2(rV)^2]^{\frac{1}{2}} \tag{21d}$$

$$w' = \{mrV/[\psi^2 + \Delta^2(rV)^2]^{\frac{1}{2}} - z'\}/\varepsilon^2$$
$$+ \Delta^2 V\{m - \nu r\psi'/[\psi^2 + \Delta^2(rV)^2]^{\frac{1}{2}}\} \tag{22}$$

where

$$m = (1 + \Delta^2 z'^2)^{\frac{1}{2}}, \qquad V = -\left(\int_0^r rq\,\mathrm{d}r\right)\Big/ r \tag{23}$$

Equations (21) reduce to the respective forms

$$\psi = rV/z' = \psi_0 \tag{24a}$$

$$T_r = m\psi_0/r \tag{24b}$$

$$T_\theta = \psi_0'/m \tag{24c}$$

$$u = r\psi_0'/m - \nu m\psi_0 \tag{24d}$$

when $\varepsilon$ is formally equated to zero. These are the forms consistent with the usual linear membrane solution (for instance, by Kraus[22]). Equation (22) becomes indeterminate for $\varepsilon = 0$. This is resolved by evaluating the terms multiplied by $\varepsilon$ in Eq. (21a) using Eq. (24a),

solving the resulting algebraic equation for $\psi$, substituting the solution into Eq. (22), expanding the result for $\varepsilon \ll 1$, and formally equating $\varepsilon$ to zero in the expression thus obtained to get

$$w_0' = -r\Big[\psi_0'' + (1/r - m'/m)\psi_0' - (m^4/r^2 + \nu m m'/r)\psi_0\Big]\Big/(mz') \tag{25}$$

This is the correct linear membrane result. Thus, all of the governing equations reduce to the correct linear membrane forms when an appropriate limiting process is used for $\varepsilon \ll 1$ (low loading). The magnitude of load consistent with low loading increases with the depth of the membrane. Although not apparent from the present work, the linear membrane problem is statically determinate and Eqs. (24) can be obtained in a much more direct way by taking this into account.

Four previous analytical investigations[2,4,10,11] of the edge effect have been performed for shallow membrane caps. For this situation $\Delta$ may be formally equated to zero in Eqs. (21) and (22) yielding

$$\varepsilon^2(\psi'' + \psi'/r - \psi/r^2) - [z'^2 - (rV/\psi)^2]/(2r) = 0 \tag{26a}$$

$$T_r = \psi/r \tag{26b}$$

$$T_\theta = \psi' \tag{26c}$$

$$u = r\psi' - \nu\psi \tag{26d}$$

$$w' = mrV/(\varepsilon^2\psi) - z' \tag{27}$$

Whereas previous derivations of Eqs. (26) and (27) were based on equations that had been simplified for moderately large deflections, the present analysis shows that the same result occurs if this simplification is not made. Note that one of the effects of invoking the simplifications mentioned at the beginning of this section is to allow existing edge effect analysis of shallow caps undergoing moderately large deflections to be extended to deep caps undergoing arbitrarily large deflections in a straightforward manner.

The development of a solution that is correct for $\varepsilon \ll 1$ and differs from the linear membrane solution only in the immediate vicinity of $r = 1$ is facilitated by the decomposition

$$\psi = \psi_0 + \varepsilon F \tag{28}$$

and the introduction of a new variable $\xi$ through

$$r = 1 - \varepsilon\xi \tag{29}$$

This is an example of a singular perturbation problem [because $\varepsilon$ multiplies the highest derivatives appearing in Eq. (21a)] but, because only a uniformly valid first approximation for $\varepsilon \ll 1$ is sought herein, many of the formalities of singular perturbation methods can be dispensed with.

Substituting Eqs. (28) and (29) into Eq. (21a), expanding all functions in the result containing $\varepsilon$ in appropriate Taylor's series for $\varepsilon \ll 1$, and formally equating $\varepsilon$ to zero in the final expression yields

$$\overset{\circ\circ}{F} - s^2 F = 0 \tag{30}$$

where

$$s = \{z'^3(1)/[V(1)m(1)]\}^{\frac{1}{2}} \tag{31}$$

Equations (30) and (31) hold for a membrane cap of any shape.

Equation (31) reduces to

$$s = [z'^3(1)/V(1)]^{\frac{1}{2}} \tag{32}$$

for a shallow cap ($\Delta \ll 1$). This is consistent with the results of Refs. 2, 4, 10, and 11. In fact, if the procedure described in the preceding paragraph is applied to Eq. (26a), Eq. (32) will emerge directly. Thus, the edge effect analysis of the shallow cap is included in that for the deep cap.

Solving Eq. (30) and taking into account that the edge effect should be confined to the immediate vicinity of $\xi = 0 (r = 1)$ produces

$$F = c\exp[-s(1 - r)/\varepsilon] \tag{33}$$

where Eq. (29) has been used. Substituting Eq. (33) into Eq. (28) yields

$$\psi = \psi_0 + \varepsilon c\exp[-s(1 - r)/\varepsilon] \tag{34}$$

which is a uniformly valid first approximation for the stress function. Substituting Eq. (34) into Eqs. (21) and (22), expanding all quantities containing $\varepsilon$ (except exponentials) in appropriate Taylor's series for $\varepsilon \ll 1$, and retaining only those associated with the linear membrane solution and the largest corresponding edge effect term yields

$$T_r = m\psi_0/r + \varepsilon c\exp[-s(1 - r)/\varepsilon]/m(1) \tag{35a}$$

$$T_\theta = \psi_0'/m + cs\exp[-s(1 - r)/\varepsilon]/m(1) \tag{35b}$$

$$u = r\psi_0'/m - \nu m\psi_0 + cs\exp[-s(1 - r)/\varepsilon]/m(1) \tag{35c}$$

$$w' = -r\Big[\psi_0'' + (1/r - m'/m)\psi_0' - (m^4/r^2 - \nu m m'/r)\psi_0\Big]\Big/ (mz') - cs^2\exp[-s(1 - r)/\varepsilon]/[\varepsilon m(1)z'(1)] \tag{35d}$$

The constant $c$ is found by specifying some combination of $T_r$ and $u$ at $r = 1$. The simplest cases are

$$T_r(1) = T_0, \qquad u(1) = u_0 \tag{36}$$

for which $c$ assumes the respective forms

$$c = m(1)[T_0 - m(1)\psi_0(1)]/\varepsilon \tag{37}$$

$$c = \Big[m(1)u_0 - \psi_0'(1) + \nu m^2(1)\psi_0(1)\Big]\Big/s \tag{38}$$

The integration of Eq. (35d) will produce one additional constant, which is found from

$$w(1) = 0 \tag{39}$$

Note that the edge effect on which the present work is predicated will occur for a prescribed radial stress resultant at the boundary only if the difference between this quantity and its linear membrane counterpart is small.

Equations (35) hold for any cap shape, any radial support conditions, and any axial force resultant produced by an axial loading per unit of projected area. An interesting special case is discussed next.

## Representative Results

As a concrete example of the solution just obtained, consider

$$q = r^\alpha, \qquad z = 1 - r^\beta \tag{40}$$

where $\alpha \geq 0$ and $\beta \geq 1$. The corresponding load nondimensionalizing factor appearing in Eqs. (19) is $V_0 = aq_0$. Combining Eqs. (23), (24a), (31), (35), (37), (38), and (40) leads to

$$T_r = [1 + (\Delta\beta r^{\beta-1})^2]^{\frac{1}{2}} r^{\alpha-\beta+2}/[(\alpha + 2)\beta] + \varepsilon c\exp[-s(1 - r)/\varepsilon]/[1 + (\Delta\beta)^2]^{\frac{1}{2}} \tag{41a}$$

$$T_\theta = (\alpha - \beta + 3)r^{\alpha-\beta+2}/\{(\alpha + 2)\beta[1 + (\Delta\beta r^{\beta-1})^2]^{\frac{1}{2}}\} + cs\exp[-s(1 - r)/\varepsilon]/[1 + (\Delta\beta)^2]^{\frac{1}{2}} \tag{41b}$$

$$u = \{(\alpha - \beta + 3)/[1 + (\Delta\beta r^{\beta-1})^2]^{\frac{1}{2}} - \nu[1 + (\Delta\beta r^{\beta-1})^2]^{\frac{1}{2}}\}r^{\alpha-\beta+3}/[(\alpha + 2)\beta] + cs\exp[-s(1 - r)/\varepsilon]/[1 + (\Delta\beta)^2]^{\frac{1}{2}} \tag{41c}$$

$$w' = \{(\alpha-\beta+3)^2/[1+(\Delta\beta r^{\beta-1})^2]^{\frac{1}{2}} - [1+(\Delta\beta r^{\beta-1})^2]^{\frac{3}{2}}\}r^{\alpha-2\beta+3}/[(\alpha+2)\beta^2] + \{(\alpha-\beta+3)/[1+(\Delta\beta r^{\beta-1})^2]^{\frac{3}{2}} + \nu/[1+(\Delta\beta r^{\beta-1})^2]^{\frac{1}{2}}\}\Delta^2(\beta-1)r^{\alpha+1}/(\alpha+2) + cs^2\exp[-s(1-r)/\varepsilon]/\{\beta[1+(\Delta\beta)^2]^{\frac{1}{2}}\varepsilon\} \quad (41d)$$

where

$$s = \{(\alpha+2)\beta^3/[1+(\Delta\beta)^2]^{\frac{1}{2}}\}^{\frac{1}{2}} \quad (42)$$

$$c = [1+(\Delta\beta)^2]^{\frac{1}{2}}\left\{T_0 - [1+(\Delta\beta)^2]^{\frac{1}{2}}/[(\alpha+2)\beta]\right\}/\varepsilon \quad (43)$$

when the edge radial stress resultant is specified, whereas

$$c = \left([1+(\Delta\beta)^2]^{\frac{1}{2}}u_0 - \{\alpha-\beta+3-\nu[1+(\Delta\beta)^2]\}/[(\alpha+2)\beta]\right)/s \quad (44)$$

when the edge radial displacement is specified. Although Eqs. (41–44) are formally correct for all values of $\alpha \geq 0$ and $\beta \geq 1$, note that regularity at $r=0$ is maintained only for certain combinations of $\alpha$ and $\beta$.

The indicated integration of Eq. (41d) required to determine the axial displacement $w$ cannot be carried out in closed-form for arbitrary values of $\alpha$, $\beta$, and $\Delta$. Three situations for which closed-form integration is possible are $\Delta=0$ (shallow cap) for which

$$w = -((\alpha-\beta+2)(\alpha-\beta+4)(1-r^{\alpha-2\beta+4})/[(\alpha+2)(\alpha-2\beta+4)\beta^2] + c[(\alpha+2)\beta]^{\frac{1}{2}}\{1-\exp[-s(1-r)/\varepsilon]\}) \quad (45a)$$

with

$$s = [(\alpha+2)\beta^3]^{\frac{1}{2}} \quad (45b)$$

and $\beta=1$ (conical cap) for which

$$w = -([1/(1+\Delta^2)^{\frac{1}{2}} - (1+\Delta^2)^{\frac{3}{2}}(\alpha+2)^2](1-r^{\alpha+2}) + c(\alpha+2)^{\frac{1}{2}}\{1-\exp[-s(1-r)/\varepsilon]\}/(1+\Delta^2)^{\frac{1}{4}}) \quad (46a)$$

with

$$s = (\alpha+2)/(1+\Delta^2)^{\frac{1}{2}})^{\frac{1}{2}} \quad (46b)$$

and $\alpha=0$ and $\beta=2$ (uniformly loaded paraboloidal cap) for which

$$w = ((1+\nu)\{[1+(2\Delta)^2]^{\frac{1}{2}} - [1+(2\Delta r)^2]^{\frac{1}{2}}\} + 1/[1+(2\Delta r)^2]^{\frac{1}{2}} - 1/[1+(2\Delta)^2]^{\frac{1}{2}})/8 + [(1+(2\Delta)^2]^{\frac{3}{2}} - [1+(2\Delta r)^2)^{\frac{3}{2}}]/24 - 2c\{1-\exp[-s(1-r)/\varepsilon]\}/[1+(2\Delta)^2]^{\frac{3}{4}} \quad (47a)$$

with

$$s = 4/[1+(2\Delta)^2]^{\frac{1}{4}} \quad (47b)$$

Greschik et al.[1] investigated the effects of radial edge displacements on paraboloidal caps characterized by a focal length $f$, a diameter $D$, and a nominal stress at the cap's center $\sigma_{ctr}$. In the present notation

$$\Delta = D/(8f), \qquad \varepsilon = (16f/D)(\sigma_{ctr}/E)^{\frac{1}{2}} \quad (48)$$

Figure 2 shows the parametric combinations considered in Ref. 1 and the corresponding parametric combinations in the present notation. The shaded part of Fig. 2 identifies the values of $\varepsilon$ that it was felt could legitimately be regarded as small. It is only for these cases that the present analysis has validity.

| $\frac{f}{D}$ / ($\Delta$) / $\frac{\sigma_{ctr}}{E}\times10^4$ | 0.25 (0.5) | 0.5 (0.25) | 0.75 (0.167) | 1.0 (0.125) | 1.5 (0.083) | 2.0 (0.063) | 4.0 (0.031) |
|---|---|---|---|---|---|---|---|
| 1.5625 | 0.05 | 0.1 | 0.15 | 0.2 | 0.3 | 0.4 | 0.8 |
| 3.125 | 0.0707 | 0.1414 | 0.2121 | 0.2828 | 0.4243 | 0.5657 | 1.134 |
| 6.25 | 0.1 | 0.2 | 0.3 | 0.4 | 0.6 | 0.8 | 1.6 |
| 12.5 | 0.1414 | 0.2828 | 0.4243 | 0.5657 | 0.8485 | 1.1314 | 2.2627 |
| | $\varepsilon$ | | | | | | |

**Fig. 2 Dimensionless $\Delta$ and $\varepsilon$ vs dimensionless parameters $f/D$ and $\sigma_{ctr}/E$.**

Greschik et al.[1] characterized radial edge displacements by a parameter $\Delta R/R$. In the present notation, the maximum absolute value of the radial edge displacement is

$$|u_0|_{max} = 8|\Delta R/R|/(\Delta\varepsilon)^2 \quad (49)$$

Note that there are two differences between the problem under consideration here and that discussed in Ref. 1. First the loading in the present case is an axial force per unit of projected area, whereas that of Ref. 1 is a normal force per unit of deformed area (pressure). These loadings are not equivalent for the larger values of $\Delta$ shown in Fig. 2. Second, the present work deals with caps having initial paraboloidal shape, whereas that of Ref. 1 is concerned with caps having final paraboloidal shape. Thus, complete correspondence between the present results and those reported by Greschik et al.[1] is not expected. Parametric combinations suggested in Ref. 1 are employed here merely as representative of a current aerospace application.

For $\alpha=0$ and $\beta=2$ the combination of Eqs. (41a–41c), (44), and (47) leads to

$$T_r = \left[[1+(2\Delta r)^2]^{\frac{1}{2}} + \varepsilon[1+(2\Delta)^2]^{\frac{1}{4}}\left(u_0 - \{1/[1+(2\Delta)^2]^{\frac{1}{2}} - \nu[1+(2\Delta)^2]^{\frac{1}{2}}\}/4\right)\exp\left(-4(1-r)/\{[1+(2\Delta)^2]^{\frac{1}{4}}\varepsilon\}\right)\right]/4 \quad (50a)$$

$$T_\theta = \left[1/[1+(2\Delta r)^2]^{\frac{1}{2}} + \left(4u_0 - \{1/[1+(2\Delta)^2]^{\frac{1}{2}} - \nu[1+(2\Delta)^2]^{\frac{1}{2}}\}\right)\exp\left(-4(1-r)/\{[1+(2\Delta)^2]^{\frac{1}{4}}\varepsilon\}\right)\right]/4 \quad (50b)$$

$$u = \left[\{1/[1+(2\Delta r)^2]^{\frac{1}{2}} - \nu[1+(2\Delta r)^2]^{\frac{1}{2}}\}r + \left(4u_0 - \{1/[1+(2\Delta)^2]^{\frac{1}{2}} - \nu[1+(2\Delta)^2]^{\frac{1}{2}}\}\right) \times \exp\left(-4(1-r)/\{[1+(2\Delta)^2]^{\frac{1}{4}}\varepsilon\}\right)\right]/4 \quad (50c)$$

$$w = \left[(1+\nu)\{[1+(2\Delta)^2]^{\frac{1}{2}} - [1+(2\Delta r)^2]^{\frac{1}{2}}\} + 1/[1+(2\Delta r)^2]^{\frac{1}{2}} - 1/[1+(2\Delta)^2]^{\frac{1}{2}} + \{[1+(2\Delta)^2]^{\frac{3}{2}} - [1+(2\Delta r)^2]^{\frac{3}{2}}\}/3 - \left(4u_0 - \{1/[1+(2\Delta)^2]^{\frac{1}{2}} - \nu[1+(2\Delta)^2]^{\frac{1}{2}}\}\right) \times \left(1-\exp\{-4(1-r)/[1+(2\Delta)^2]^{\frac{1}{4}}\varepsilon\}\right)\right]/8 \quad (50d)$$

Equations (20) and (50) [and, of course, the more general Eqs. (41) of which Eqs. (50) are special cases] illustrate analytically several important trends. The exponentials appearing in Eqs. (50) are associated with the edge effect. All terms containing the radial edge displacement $u_0$ are multiplied by such exponentials in Eqs. (50a–50c). Thus, the central region in which the stress resultants and radial displacements are unaffected by radial edge displacements (unaffected region) decreases with increasing $\varepsilon$. According to Eq. (20b), the unaffected region is minimized for shallow caps and high loads. Equation (50d), on the other hand, contains a factor of $-u_0/2$ not multiplied by an exponential. This represents a rigid axial displacement of the unaffected region with no shape change. Thus, the edge effect protects the shape of the unaffected region from radial edge displacements.

The trends discussed in the preceding paragraph were deduced by Greschik et al.[1] from their numerical solutions. The numerical and analytical approaches are complementary in the sense that the former is not limited to small values of $\varepsilon$, whereas the latter is capable of producing explicit results ($\varepsilon$ proportional to $V_0^{1/2}$ and $\Delta^{-3/2}$, rigid axial displacement equal to $-u_0/2$, etc.). Recall that the loading employed here is different than that considered in Ref. 1. This suggests that the basic elements of edge effect behavior are pertinent to a variety of loadings.

Figures 3–10 show representative numerical results based on Eqs. (50) corresponding to the entry in the upper left-hand corner of Fig. 2 and $\nu = 0.3$ (to be consistent with Ref. 1). Figures 3–6 show results for the edge fixed against radial displacement, whereas Figs. 7–10 show the effect of imposing the largest outward and inward radial edge displacements as determined from Eq. (49) based on the value $\Delta R/R = 0.0024$ given in Ref. 1. In Figs. 3–5, the linear membrane (LM) solution is identified. Two versions of the LM axial displacement are given in Fig. 6. The first ($LM_1$) corresponds to vanishing of the edge radial displacement, whereas the second ($LM_2$) corresponds to vanishing of the edge tangential displacement. This illustrates the fact that (unlike the LM results for the stress resultants and the radial displacement) the LM solution for the axial displacement depends on the form of boundary support. It is version $LM_2$, incidentally, that is normally presented in standard references such as Kraus.[22]

It can be seen that values of the stress resultants and the radial displacement conform to the LM solution except in the immediate vicinity of the edge for all radial edge displacements. The axial displacement in the interior of the cap is affected by radial edge displacements, but the effect is equivalent to a rigid axial displacement:

$$W = -u_0/2 + \{1/[1 + (2\Delta)^2]^{\frac{1}{2}} - \nu[1 + (2\Delta)^2]^{\frac{1}{2}}\}/8 \qquad (51)$$

[as can be seen from Eq. (50d)].

The $T_\theta$ results corresponding to the inward radial edge displacement show a compression region. These predictions are unrealistic for the types of membranes used in aerospace applications in which wrinkling (not included in the present model), rather than

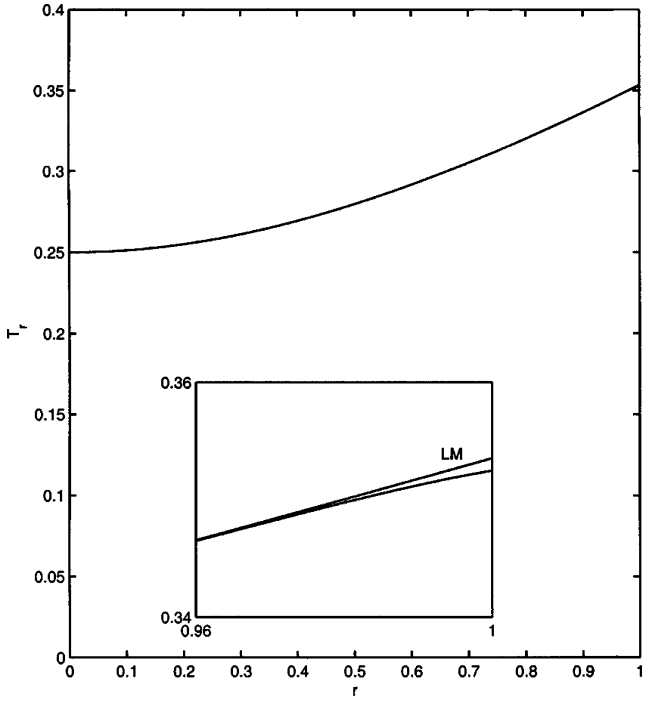


**Fig. 3 Radial stress resultant profiles, $f/D = 0.25$, $\sigma_{ctr}/E = 1.5625 \times 10^{-4}$, and $u_0 = 0$.**

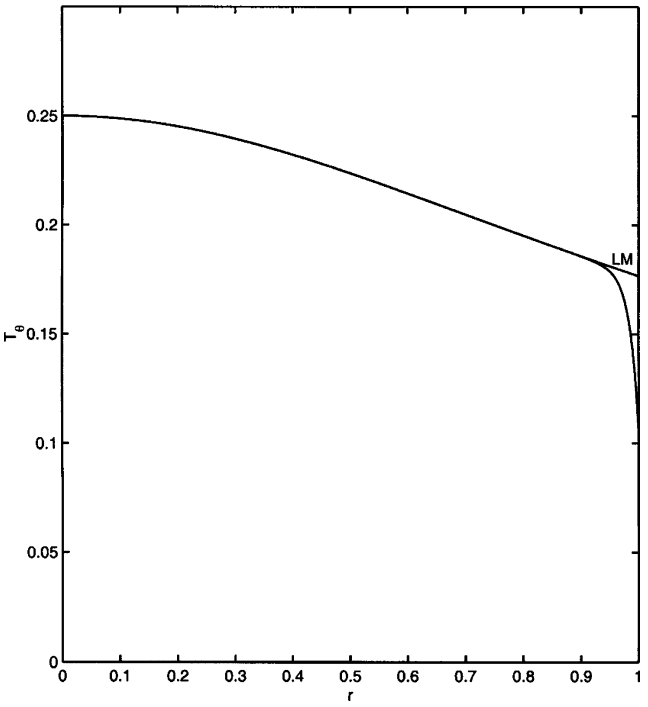


**Fig. 4 Transverse stress resultant profiles, $f/D = 0.25$, $\sigma_{ctr}/E = 1.5625 \times 10^{-4}$, and $u_0 = 0$.**

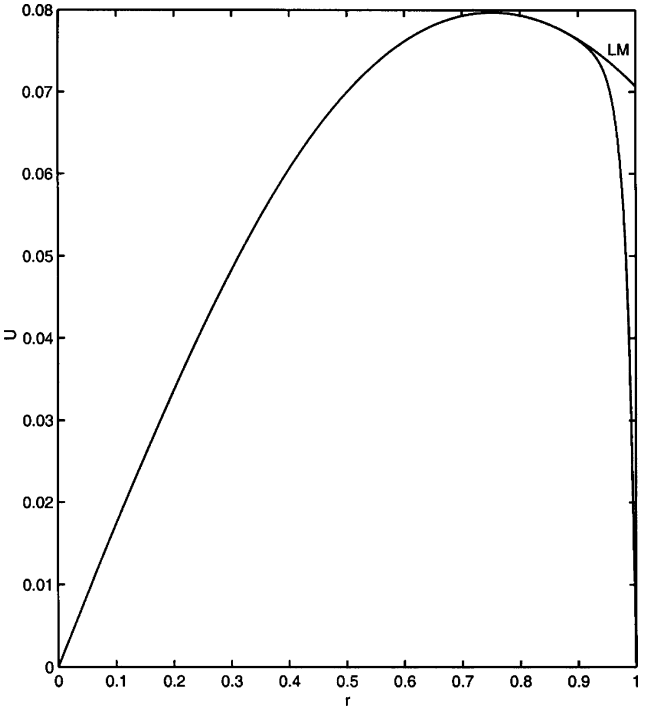


**Fig. 5 Radial displacement profiles, $f/D = 0.25$, $\sigma_{ctr}/E = 1.5625 \times 10^{-4}$, and $u_0 = 0$.**

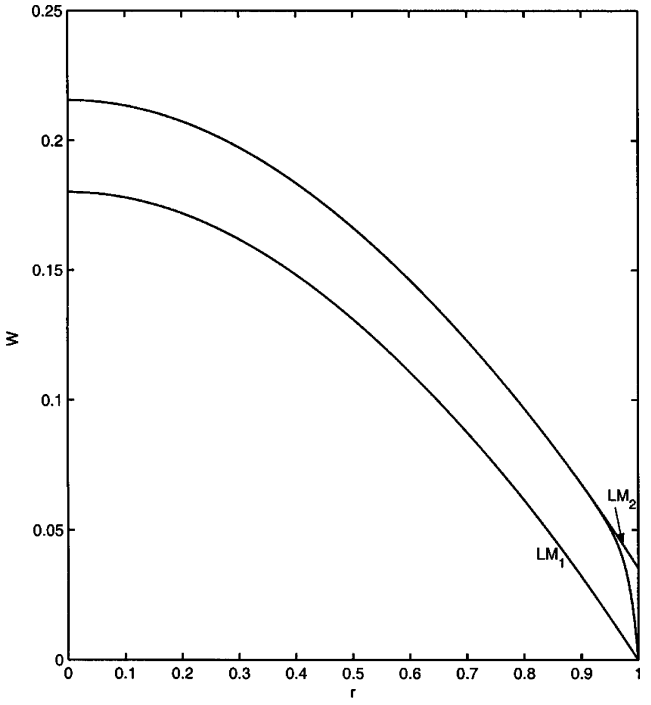


**Fig. 6 Axial displacement profiles, $f/D = 0.25$, $\sigma_{ctr}/E = 1.5625 \times 10^{-4}$, and $u_0 = 0$.**

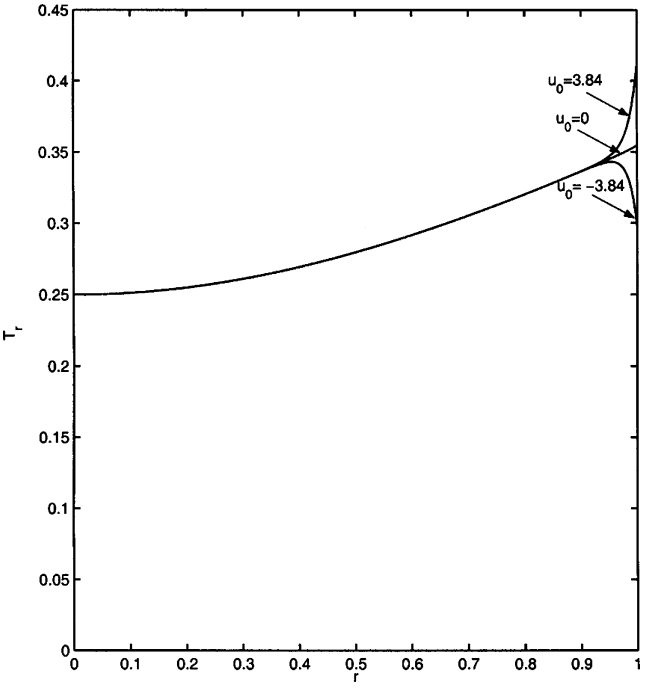


**Fig. 7 Radial stress resultant profiles, $f/D = 0.25$ and $\sigma_{ctr}/E = 1.5625 \times 10^{-4}$.**

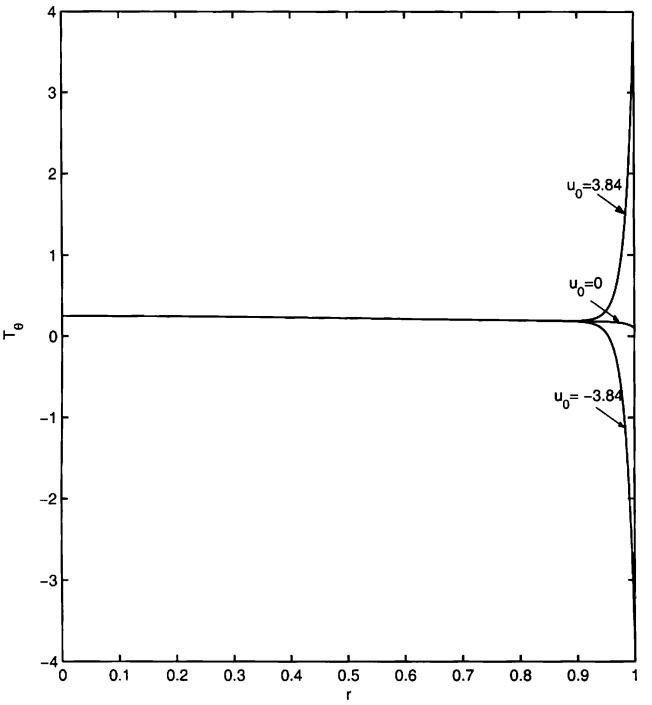


**Fig. 8 Transverse stress resultant profiles, $f/D = 0.25$ and $\sigma_{ctr}/E = 1.5625 \times 10^{-4}$.**

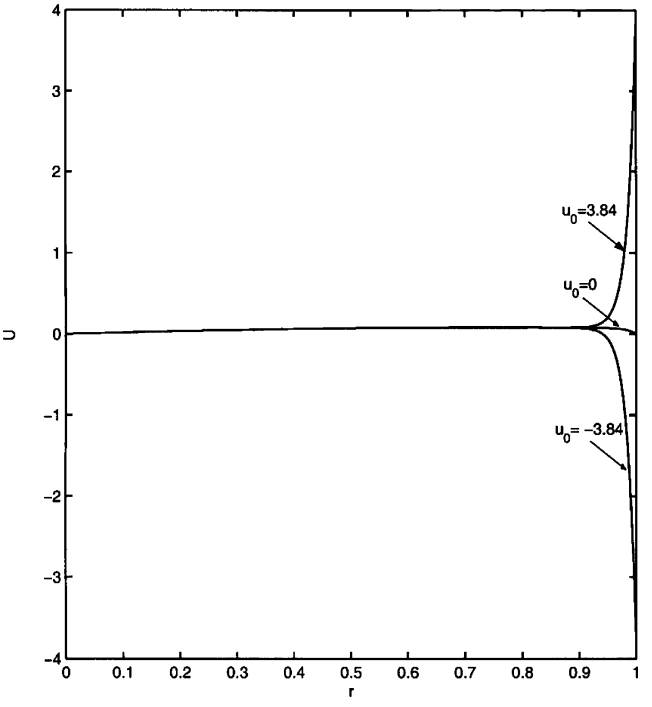


**Fig. 9 Radial displacement profiles, $f/D = 0.25$ and $\sigma_{ctr}/E = 1.5625 \times 10^{-4}$.**

compression, would occur. Such results could be realistic, however, for the concrete caps used in structural applications.

Conceptually, it is not difficult to incorporate a wrinkling model into a membrane deformation analysis. One way of doing this is discussed by Greschik et al.[1] It was felt, however, that the inclusion of a wrinkling model would unduly complicate the edge effect analysis, which is the primary subject of the present paper. For this reason, a wrinkling model was omitted herein.

## Alternate Asymptotic Analysis

Dickey,[7] in the context of moderately large deflections of shallow caps, proposed a set of linear equations containing the edge effect. A method similar to that in Ref. 7 is applied to Eqs. (21) and (22) in this section. The resulting linearized equations serve as an alternative to the edge effect formulation discussed earlier.

The starting points of the linearization are the decomposition

$$\psi = \psi_0 + \Delta\psi \tag{52}$$

and the assumption $\Delta\psi \ll \psi_0$. Thus, the linearization is being performed about the LM solution. Substituting Eq. (52) into Eqs. (21) and (22), consistently expanding all nonlinear terms for $\Delta\psi/\psi_0 \ll 1$, neglecting all terms nonlinear in $\Delta\psi/\psi_0$, and eliminating $\Delta\psi$ in

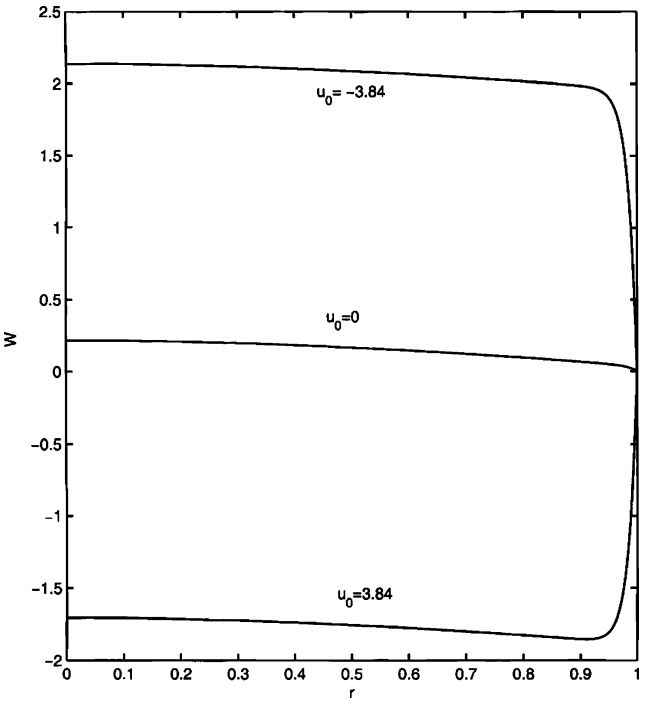


**Fig. 10 Axial displacement profiles, $f/D = 0.25$ and $\sigma_{ctr}/E = 1.5625 \times 10^{-4}$.**

favor of $\psi$ from the final results using Eq. (52) leads to

$$\varepsilon^2[\psi'' + (1/r - m'/m)\psi' - m^2\psi/r^2] + z'\{z'(1 - \psi/\psi_0) + \nu\varepsilon^2\Delta^2(z'\psi_0)'[\psi/\psi_0 - (1 + m^2)]/m\}/(mr) = 0 \tag{53a}$$

$$T_r = [\psi + (m^2 - 1)\psi_0]/(mr) \tag{53b}$$

$$T_\theta = \psi'/m \tag{53c}$$

$$u = \{r\psi' - \nu[\psi + (m^2 - 1)\psi_0]\}/m \tag{53d}$$

$$w' = z'\Big((1 - \psi/\psi_0)\Big/(m\varepsilon)^2 + \Delta^2\{m\psi_0/r + \nu\big[\psi_0'(\psi/\psi_0 - 1)\Big/m^2 - \psi'\big]\Big/m\}\Big) \tag{53e}$$

Equations (53) constitute the linearized forms of Eqs. (21) and (22) and generalize the analysis reported by Dickey[7] to a formulation correct for deep caps, arbitrarily large deflections, and axial loads per unit of projected area. It can be shown, by taking appropriate limits, that Eqs. (53) contains both the LM equations and the edge effect equations developed earlier. The formulation described by Eqs. (53) is, thus, an alternative to that discussed earlier.

Equation (53a) is linear with variable coefficients. Numerical solutions of Eq. (53a) can, therefore, be carried out without iteration. This makes Eq. (53a) a useful model equation to test the ability of proposed numerical methods to deal with the edge effects expected for $\varepsilon \ll 1$. Such tests can play an important role in the verification of computational approaches. In addition, Eq. (53a), being formally valid for any value of $\varepsilon$, can be used to study the range of values of $\varepsilon$ for which the edge effect formulation would be of utility. A specific example of this kind is discussed next.

Consider the closed-form solution to Eq. (53) reported by Dickey[7] for $\alpha = 0$, $\beta = 2$, and $\Delta \ll 1$ (shallow paraboloidal cap subjected to uniform loading). For the special case of an edge fixed against radial displacement, the results of Ref. 7 (written in the present notation) reduce to

$$T_r = \{1 - (1 - \nu)\varepsilon I_1(4r/\varepsilon)/(4r)/[I_0(4/\varepsilon) - \varepsilon(1 + \nu)I_1(4/\varepsilon)/4]\}/4$$

$$T_\theta = \{1 - (1 - \nu)[I_0(4r/\varepsilon) - \varepsilon I_1(4r/\varepsilon)/(4r)]/[I_0(4/\varepsilon) - \varepsilon(1 + \nu)I_1(4/\varepsilon)/4]\}/4$$

$$u = (1 - \nu)r\{1 - [I_0(4r/\varepsilon) - \varepsilon(1 + \nu)I_1(4r/\varepsilon)/(4r)]/[I_0(4/\varepsilon) - \varepsilon(1 + \nu)I_1(4/\varepsilon)/4]\}/4$$

$$w = (1 - \nu)[I_0(4/\varepsilon) - I_0(4r/\varepsilon)]/\{8[I_0(4/\varepsilon) - \varepsilon(1 + \nu)I_1(4/\varepsilon)/4]\} \tag{54}$$

Formally expanding Eqs. (54) for $\varepsilon \ll 1$ using the appropriate asymptotic forms of $I_0$ and $I_1$ for large arguments produces

$$T_r = \{1 - \varepsilon(1 - \nu)\exp[-4(1 - r)/\varepsilon]/4\}/4$$

$$T_\theta = \{1 - (1 - \nu)\exp[-4(1 - r)/\varepsilon]\}/4$$

$$u = (1 - \nu)\{r - \exp[-4(1 - r)/\varepsilon]\}/4$$

$$w = (1 - \nu)\{1 - \exp[-4(1 - r)/\varepsilon]\}/8 \tag{55}$$

Equations (55) are written so that the first term of each is the LM solution, whereas the second is the largest edge effect correction. All terms containing exponentials have been simplified by recognizing that they will vanish except in the immediate vicinity of $r = 1$ for $\varepsilon \ll 1$ and simplifying all other functions of $r$ appearing therein accordingly. Doing this creates expressions that all are identical to the special cases of Eqs. (50) corresponding to $\alpha = 0$, $\beta = 2$, $u_0 = 0$, and $\Delta \ll 1$. Comparison of Eqs. (54) and (55) can provide information about the upper limit of $\varepsilon$ for which the latter will provide a reasonable approximation to the former.

## Conclusions

An analysis of the edge effect in membrane cap axisymmetric deformations was carried out based on equations that are correct for arbitrarily large deflections of caps exhibiting a form of linearly elastic response and subjected to axial loads per unit of projected area. It was shown that the problem could be formulated to produce a single nonlinear ordinary differential equation governing a stress function and that this formulation provided a convenient context for extending the edge effect analysis initiated by Bromberg and Stoker[2] using equations correct for moderately large deflections of shallow caps to equations correct for arbitrarily large deflections of deep caps.

It was found that the edge effect analysis facilitated the development of rather general closed-form solutions for arbitrary cap shapes and loadings. A subclass of these solutions was used to provide an analytical example of the phenomenon of protection of the interior shape of the membrane from edge displacements observed in previous numerical solutions and to demonstrate that this phenomenon is insensitive to the details of loading.

As an alternative to edge effect analysis, a different asymptotic analysis, suggested by Dickey,[7] was extended to equations correct for arbitrarily large deformations. A consistency was demonstrated between the results of the two methodologies, and ways in which both could be used as parts of the verification process for numerical methods were discussed.

## References

[1]Greschik, G., Palisoc, A., Cassapakis, C., Veal G., and Mikulas, M. M., "Sensitivity Study of Precision Pressurized Membrane Reflector Deformations," *AIAA Journal*, Vol. 39, No. 2, 2001, pp. 308–314.

[2]Bromberg, E., and Stoker, J. J., "Non-Linear Theory of Curved Elastic Sheets," *Quarterly of Applied Mathematics*, Vol. 3, No. 3, 1945, pp. 246–265.

[3]Hencky, H., "Über den Spannungszustand in Kreisruden Platten mit Verschwindender Biegungssteifigkeit," *Zeitschrift für Mathematik und Physik*, Vol. 63, 1915, pp. 311–317.

[4]Reissner, E., "Rotationally Symmetric Problems in the Theory of Thin Elastic Shells," *Proceedings of the Third U.S. National Congress of Applied Mechanics*, American Society of Mechanical Engineers, New York, 1958, pp. 51–69.

[5]Dickey, R. W., "The Plane Circular Elastic Surface Under Normal Pressure," *Archive for Rational Mechanics and Analysis*, Vol. 26, No. 2, 1967, pp. 219–236.

[6]Dickey, R. W., "Membrane Caps," *Quarterly of Applied Mathematics*, Vol. 45, No. 4, 1987, pp. 697–712.

[7]Dickey, R. W., "Membrane Caps Under Hydrostatic Pressure," *Quarterly of Applied Mathematics*, Vol. 46, No. 1, 1988, pp. 95–104.

[8]Dickey, R. W., "Rotationally Symmetric Solutions for Shallow Membrane Caps," *Quarterly of Applied Mathematics*, Vol. 47, No. 3, 1989, pp. 571–581.

[9]Yang, W. H., and Feng, W. W., "On Axisymmetrical Deformations of Nonlinear Membranes," *Journal of Applied Mechanics*, Vol. 92, No. 4, 1970, pp. 1002–1011.

[10]Smith, D. G., Peddieson, J., and Chung, C. J., "Finite Deflection of a Shallow Spherical Membrane," *AIAA Journal*, Vol. 11, No. 5, 1973, pp. 736–738.

[11]Chang, W., and Peddieson, J., "Large Deflections of a Shallow Conical Membrane," *Proceedings of the 13th Annual Meeting of the Society of Engineering Science*, Vol. 2, NASA Langley Research Center, Hampton, VA, 1976, pp. 575–584.

[12]Fan, S., and Peddieson, J., "Symmetric Moderately Large Deformations of a Shallow Spherical Membrane by Edge Loads," *Letters in Applied and Engineering Science*, Vol. 22, No. 6, 1984, pp. 781–788.

[13]Foroutan-Naini, F., and Peddieson, J., "Large Axisymmetric Deformations of Elastic Circular Membranes," *Mechanics Research Communications*, Vol. 11, No. 1, 1984, pp. 67–74.

[14]Tseng, C., and Peddieson, J., "Arbitrarily Large Deflections of Circular Membranes Due to Transverse Loading," *Industrial Mathematics*, Vol. 34, No. 2, 1984, pp. 181–191.

[15]Kyriakides, S., and Chang, Y., "The Initiation and Propagation of a Localized Instability in an Inflated Elastic Tube," *International Journal of Solids and Structures*, Vol. 27, No. 9, 1991, pp. 1085–1111.

[16]Khayat, R. E., Derdouri, A., and Garcia-Rèjon, A., "Inflation of an Elastic Cylindrical Membrane: Non-Linear Deformation and Instability," *International Journal of Solids and Structures*, Vol. 29, No. 1, 1992, pp. 69–87.

[17]Foroudastan, S., and Peddieson, J., "Large Axisymmetric Deformation of an Elastic Cylindrical Membrane due to Combined Loading," *Industrial Mathematics*, Vol. 42, No. 2, 1992, pp. 49–66.

[18]Weinitschke, H. J., and Grabmüller, H., "Recent Mathematical Results in the Nonlinear Theory of Flat and Curved Elastic Membranes of Revolution," *Journal of Engineering Mathematics*, Vol. 26, No. 1, 1992, pp. 159–194.

[19]Khayat, R. E., and Derdouri, A., "Inflation of a Hyperelastic Cylindrical Membranes as Applied to Blow Molding. Part I. Axisymmetric Case," *International Journal for Numerical Methods in Engineering*, Vol. 37, No. 22, 1994, pp. 3773–3791.

[20]Bech, A., and Grabmüller, H., "On Finite Displacements of Curved Annular Membranes Without Wrinkling," *Quarterly of Applied Mathematics*, Vol. 53, No. 3, 1995, pp. 527–550.

[21]Rossettos, J. N., "Nonlinear Membrane Solutions for Symmetrically Loaded Deep Membranes of Revolution," NASA TN D-3297, March 1966.

[22]Kraus, H., *Thin Elastic Shells*, Wiley, New York, 1967.

[23]Palisoc, A. L., and Huang, Y., "Design Tool for Inflatable Space Structures," AIAA Paper 97-1378, 1997.

M. Sichel
*Associate Editor*